NRC·CNRC

NRC Publications Archive
Archives des publications du CNRC

Three-dimensional numerical model development for the investigation of the gas jet wiping process on the flow behaviors near the galvanizing bath surface

Yu, K. R.; Ilinca, F.; Blais, B.; Goodwin, F. E.

This publication could be one of several versions: author's original, accepted manuscript or the publisher's version. / La version de cette publication peut être l'une des suivantes : la version prépublication de l'auteur, la version acceptée du manuscrit ou la version de l'éditeur.

Publisher's version / Version de l'éditeur:

2018 AISTech Conference Proceedings, 2018-05

NRC Publications Record / Notice d'Archives des publications de CNRC:
https://nrc-publications.canada.ca/eng/view/object/?id=b027cd92-7e0e-4315-bce7-45e4859d60fe
https://publications-cnrc.canada.ca/fra/voir/objet/?id=b027cd92-7e0e-4315-bce7-45e4859d60fe

Access and use of this website and the material on it are subject to the Terms and Conditions set forth at
https://nrc-publications.canada.ca/eng/copyright
READ THESE TERMS AND CONDITIONS CAREFULLY BEFORE USING THIS WEBSITE.

L'accès à ce site Web et l'utilisation de son contenu sont assujettis aux conditions présentées dans le site
https://publications-cnrc.canada.ca/fra/droits
LISEZ CES CONDITIONS ATTENTIVEMENT AVANT D'UTILISER CE SITE WEB.

Questions? Contact the NRC Publications Archive team at PublicationsArchive-ArchivesPublications@nrc-cnrc.gc.ca. If you wish to email the authors directly, please see the first page of the publication for their contact information.

Vous avez des questions? Nous pouvons vous aider. Pour communiquer directement avec un auteur, consultez la première page de la revue dans laquelle son article a été publié afin de trouver ses coordonnées. Si vous n'arrivez pas à les repérer, communiquez avec nous à PublicationsArchive-ArchivesPublications@nrc-cnrc.gc.ca.

National Research Council Canada | Conseil national de recherches Canada

Canada

Three-dimensional numerical model development for the investigation of the Gas Jet Wiping process on the flow behaviors near the galvanizing bath surface

K. R. Yu[1], F. Ilinca[1], B. Blais[1], F. E. Goodwin[2]

[1] National Research Council of Canada
75 de Mortagne, Boucherville, Québec, Canada. J4B 6Y4
Phone: (450) 641-5072
Email: kintakraymond.yu@cnrc-nrc.gc.ca; florin.ilinca@cnrc-nrc.gc.ca; bruno.blais@cnrc-nrc.gc.ca;

[2] International Zinc Association
2530 Meridian Parkway, Ste. 115, Durham, NC 27713
Phone: (919) 361-4647
Email: fgoodwin@zinc.org

Keywords: Gas Jet Wiping, Continuous Galvanizing Bath, Numerical Modeling

ABSTRACT

In continuous galvanizing bath operations, the thickness and the uniformity of the zinc coating are strongly influenced by the gas jet wiping process which aims to remove the excess liquid zinc adhered to the steel strip as it emerges from the bath. This work describes the development process of a three-dimensional numerical model which aims to consider the moving strip, the turbulent jet, and their complex interactions with the falling excess liquid zinc. Such model would be highly valuable to advance the fundamental understanding of the complex flow behaviors near the bath surface.

INTRODUCTION

Maintaining a stable and uniform zinc coating on the steel strip surface in continuous galvanizing bath operations is of critical importance in achieving automotive grade steel products. As the steel strip emerges from the bath, the excess liquid zinc adhered to the strip surface is typically removed by the gas jet wiping process to obtain the desired zinc coating thickness. Although the gas wiping is safe, rather efficient and economical to operate, the process still faces several limitations; for example, the sensitivity of the nozzle to strip distance, the splashing phenomenon, the undesired formation of top skimming, etc. [1] In particular, the skimming formation increases the production cost. Hence, there is a continuous interest from the industries to improve the wiping process [2], [3]. This, in turns, demands a better understanding of the process itself.

Numerical simulation has shown to be a useful tool to gain deeper understanding of complex flow phenomena, such as the gas wiping jet process [4], [5]. To shed lights on the influence from the gas wiping process onto the formation of top skimmings, it demands to better understand the fundamental flow behaviors near the bath surface. It is therefore necessary to have an efficient three-dimensional numerical model to describe the overall gas jet wiping process near the galvanizing bath surface; considering the moving strip, the turbulent jet flow, and their complex interactions with the falling excess liquid zinc. This work describes the model development process and the associated challenges encountered during the development.

The paper is organized as follows: First, the gas jet wiping process near the galvanizing bath surface is overviewed, followed by a brief outline of the methodology of the model construction. Then, the development work and preliminary results of two sub-models, namely the gas jet wiping unit and the free surface model for the molten zinc, are presented. The paper concludes with the planned future work.

PROCESS OVERIVEW AND MODELING METHODOLOGY

Overview of the gas jet wiping process

The typical configuration of the gas jet wiping is shown in Figure 1. Right after the steel strip emerges from the galvanizing bath, the strip is guided vertically up, traveling at a speed of 50 to 200 m/min, through the gas jet wiping unit; which impinges high pressure gas onto the strip to wipe off the excess entrained liquid zinc back to the galvanizing bath [1]. Typically, the gas jet wiping unit can achieve a zinc coating layer between 5 to 30 μm [5]. The turbulent impinging gas flow interacts with the falling excess liquid zinc, and forms an unsteady free surface flow regime, beginning from the stagnation region of the impinging jet down towards the galvanizing bath surface. Three dimensional flow features can exist. The length scales involved in the process vary several orders. For example, flow dynamics at the free surface along the steel strip have a

time scale of the order of milliseconds and a length scale of tens of microns. However, for the flow inside the bath the time scale is in seconds and the length scale is in meters. It is not at all trivial to develop a numerical model to capture such a complex multiphase multiscale phenomenon.

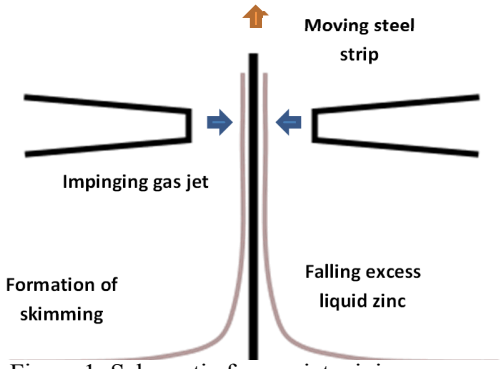

Figure 1: Schematic for gas jet wiping process

Model development methodology

The objective here is to capture the important physical phenomena for top skimming investigation in 3D with sufficient accuracies and also to maintain the efficiency of the simulation as much as possible. Previously, the gas jet wiping phenomenon has been captured rather successfully in 2D using Large Eddy Simulation (LES) for the turbulent flow, together with Volume of Fluids (VOF) for the free surface of the liquid zinc [4], [5]. Although the predictions are satisfactory, the associated computational cost is rather high and the approach is not practical for the investigation in 3D. An alternative route to develop a 3D numerical model, capturing the relevant physical phenomena is attempted in a step-by-step manner in the present work.

In the wiping process, the liquid zinc film is subjected to the influences of the pressure gradient and the shear stress from the gas jet and the surface tension of the liquid zinc. The sensitivities of these factors onto the final coating thickness is however small; even a zero-dimensional air-knife model, considering only the peak jet pressure gradient and the maximum jet shear stress with the surface tension effect ignored, can predict the final coating thickness satisfatory [6]. On the other hand, Pfeiler et al. [5] has demonstrated that the presence of the adhered zinc film on the steel strip can interact locally with the wiping gas jet and the location of the recirculation zone can be shifted slightly up towards the nozzle from the strip surface. Due to the large length scale differences between this local shift of recirculation zone and the distance towards the bath surface from the air-knife, the small local displacement of the recirculation zone is not expected to have any significant influences on the global flow behavior of the gas jet with respect to the galvanizing bath surface. Hence, in this first modeling development attempt, the wiping gas jet flow field and the adhered liquid zinc profile near the bath surface are assumed to be sufficiently weakly coupled such that they can be evaluated in a separate manner. Besides, the heat transfer between the gas and the liquid phases are also not considered.

The model construction begins with the model of the gas jet wiping unit, also commonly referred to as the air-knife. Then, the model for adhesion of liquid zinc on the moving steel strip near the galvanizing bath surface, coupled with the air-knife effect, is considered. The model development will first start in two-dimensions. Successful strategies will then be carried forward to the three-dimensional cases.

NUMERICAL MODEL

Gas jet wiping model

It is well established that the pressure and shear stress distribution generated on the liquid film by the air knives plays a critical role on the efficiency of the wiping process. These distributions depend on the configuration, which includes mainly the geometry of the air-knife, the stand-off distance and the knife angle, as well as the inlet pressure and temperature of the gas. Generally, the flow generated by the air knife remains subsonic or transonic [5]. Thus, the Mach number of most configurations can be significantly higher than 0.3, and the compressible nature of the flow significantly alters the gas-liquid interaction, as compared to the case for which both can be modeled as incompressible fluids.

Considering these elements, compressible flow simulations are required in order to determine the stress on the impinged strip surface and integrate them within the free surface simulation. These simulations should be robust and parametric to ensure the capacity to handle a variety of air knife geometry. In the present work, these simulations are carried out using SU2, which is a widely used implicit finite-volume computational fluid dynamics application [7]–[9].

First, the governing equations and their numerical discretization are briefly overviewed, followed by the meshing strategy and the validation of the obtained pressure profiles using an air knife geometry described by Alibeigi [10], from which experimental results for the pressure at the stagnation point are available.

Equations and discretization

The compressible, turbulent Reynolds-Averaged Navier-Stokes equations in conservative form are [9]:

$$\frac{\partial \mathbf{V}}{\partial t} + \nabla \cdot \mathbf{F}^c - \nabla \cdot \mathbf{F}^v - \mathbf{Q} = 0$$

$$\mathbf{V} = \left[\rho, \mathbf{u}, E\right]^T$$

The conservative variables vector $\boldsymbol{V}$ contain the density, the velocity components and the internal energy. The convective fluxes, viscous fluxes and source term are defined as [9]:

$$\mathbf{F}^c = \begin{bmatrix} \rho\mathbf{u} \\ \rho\mathbf{u}\otimes\mathbf{u} + p\mathbf{I} \\ \rho E\mathbf{u} + p\mathbf{u} \end{bmatrix}, \quad \mathbf{F}^v = \begin{bmatrix} 0 \\ \boldsymbol{\tau} \\ \boldsymbol{\tau}\cdot\mathbf{u} + k_{tot}\nabla T \end{bmatrix}$$

where ρ is the mean density, $\boldsymbol{u}$ the mean velocity vector, p the mean pressure, $\boldsymbol{I}$ the identity tensor, E the mean total energy, T the temperature and k_{tot} the total conductivity (turbulent and laminar). The viscous stress tensor $\boldsymbol{\tau}$ is defined as:

$$\boldsymbol{\tau} = \mu_{tot}\left(\nabla\mathbf{u} + \nabla\mathbf{u}^T - \frac{2}{3}\mathbf{I}\left(\nabla\cdot\mathbf{u}\right)\right)$$

The total viscosity and conductivity are computed from the laminar viscosity and the turbulent viscosity following the Boussinesq hypothesis:

$$\mu_{tot} = \mu_l + \mu_t$$

$$k_{tot} = \frac{\mu_l}{\mathrm{Pr}} + \frac{\mu_t}{\mathrm{Pr}_t}$$

where μ_l is the laminar (or dynamic) viscosity, μ_t is the turbulent viscosity, Pr is the Prandlt number and $\mathrm{Pr_t}$ is the turbulent Prandlt number. In this work, the Menter shear stress transport (SST) k-ω model is employed to compute the turbulent viscosity [11]. The present configuration is found to be not sensitive with the chosen turbulence model. In particular, no significant differences were observed as compared with another widely popular turbulence model: the Spalart-Allmaras (S-A) model [12]. An ideal gas equation of state is used and the laminar viscosity is calculated using Sutherland's law as a function of the gas temperature alone.

These equations are solved in for steady-state using an adaptive time-stepping approach until the density residual reached is below 10^{-10}. A first-order upwind scheme is used for the conservative and the turbulent variables. This scheme can introduce numerical dissipations. Such effect is compensated by using highly refined meshes. The strategy used to discretize the domain and impose the boundary conditions are discussed in sequel.

Domain and boundary conditions

The air knife flow is modeled using 2D simulations with a symmetry axis on the X axis. The dimensions of the air knife and of the domain studied are given in Table **1** and the domain is illustrated at Figure **2**. Two cases are considered where the stand-off distance to outlet height ratio is $z/d = 6$ and $z/d = 8$ respectively, with a Reynolds number of ~ 11000.

Table 1: Dimensions of the air knife model domain

Dimension	**Symbol**	**Value**
Length	L	$0.03\ m$
Height of the air-knife outlet	d	$0.0015\ m$
Height of the domain	H	$0.05\ m$
Stand-off distance	z	0.006 or $0.008\ mm$

The height of the computational domain is set to be significantly larger than the air knife height to ensure that there is no interaction between the outlet boundary conditions (at ambient pressure) and the air-knife flow. Since the experimental work of Alibeigi [10] did not report the inlet condition corresponding to the experiments, a total-pressure inlet condition was imposed where the pressure was varied until a stagnation pressure equals to that of the experiments was obtained. Thus, only the profile of the pressure will be validated and not the absolute value of the pressure because of the lack of information on the inlet conditions.

For such compressible flow simulations, great care must be taken in the mesh generation to ensure adequate wall resolution (*i.e.* $y^+ < 1$). Meshes of the domain were generated using GMSH [13] at three refinement levels. For the $z/d = 6$ case, the meshes contain 66, 99 and $135k$ quadrilateral elements, and a limited number of triangular elements (< 10); for the $z/d = 8$ cases, the meshes contain 74, 115 and $160k$ elements. Similar conclusions were drawn on the pressure profile for the two finer meshes.

No observable differences on the pressure on the wall surface could be observed between the medium and finest meshes for both the $z/d = 6$ and $z/d = 8$ cases. Thus, the finest mesh was considered to be sufficiently fine. The finest mesh used for the $z/d = 6$ case is illustrated in Figure **2**. Effort was made to ensure that there was a conformal boundary layer that was adapted to the sharp edges of the exit of the air-knife (magenta rectangle of Figure **2**) and that extended progressively towards the wall (cyan rectangle of Figure **2**).

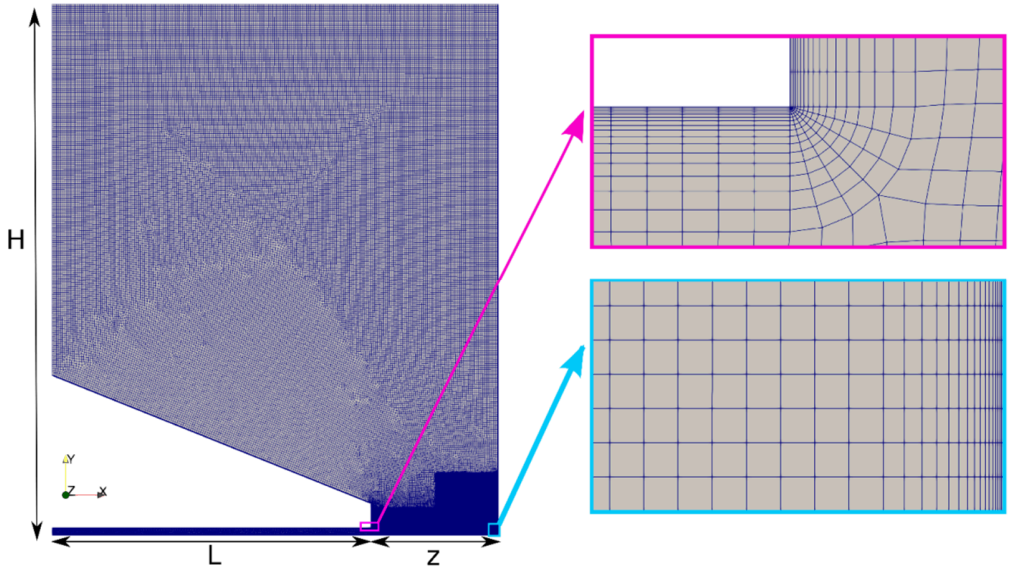

Figure 2: Illustration of one of the mesh used for the $\boldsymbol{z/d = 6}$ case. A zoom-in is provided to illustrate the fan boundary layers on the corners of the geometry and the progressiveness of the boundary layer on the sheet surface

Validation

Figure 3 presents the Mach contour and the streamlines obtained for the case $z/d = 6$ at $Re = 11000$. The size of the stagnation zone due to the build-up of the pressure close to the surface can be clearly identified.

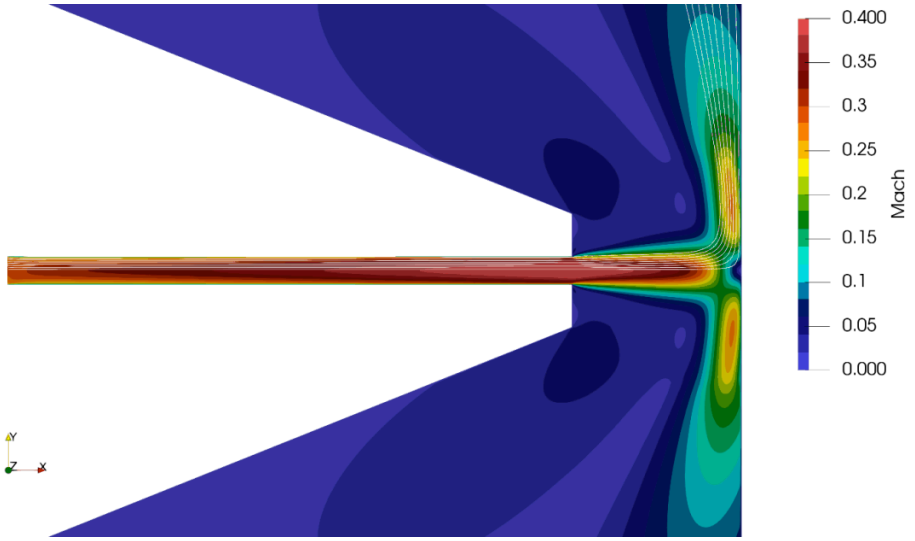

Figure 3: Mach contour and streamlines for the $\boldsymbol{z/d = 6}$ case

Figure 4 compares the results for the normalized pressure on the surface ($p/(0.5\rho U^2)$) as a function of height with the experimental results of Alibeigi [10]. Recall that the exit velocity U can be calculated for an ideal gas as a function of the stagnation pressure p_{st} [10]:

$$U = c\sqrt{\frac{2}{\gamma - 1}\left[\left(\frac{P}{P_\infty}\right)^{\frac{\gamma-1}{\gamma}} - 1\right]}$$

This normalization of the results was carried out to allow for a comparison with the results of Alibeigi [10]. Note that the jet appears to diffuse or expand more at higher stand-off distance than what is measured in the experiments. However, a very good agreement is obtained for the pressure distribution between the simulations and the experiments for both stand-off distances investigated. This is especially true considering the uncertainties surrounding the boundary conditions and the absence of error bars on the experimental results to estimate experimental uncertainties. Therefore, compressible flow simulations carried out with SU2 estimate accurately the pressure distribution on the steel strip surface. This information can now be used as an input for the film simulations.

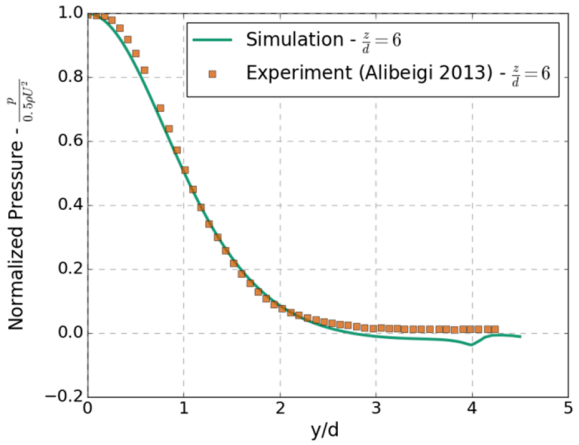

a) Case z/d=6: A very good agreement is obtained between the two results.

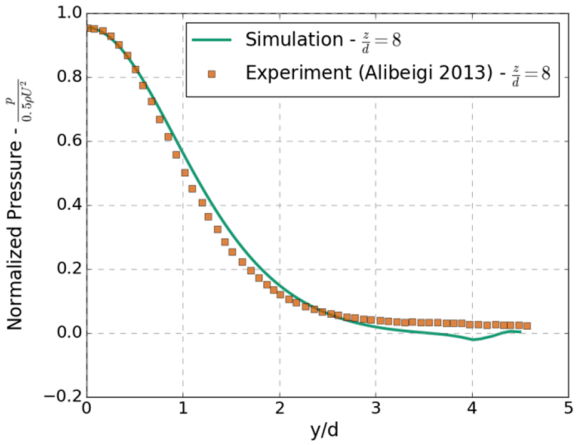

b) Case z/d=8: A good agreements is obtained, but the pressure profile appears to be slightly too wide.

Figure 4: Comparison of the normalized pressure profile between the experiments and simulation

Liquid zinc film model

To model the free surface and the flow dynamics of the liquid phase, an in-house 3D finite element flow solver is employed, using an enriched stabilized discontinuous-pressure formulation coupled with a level-set approach to describe the liquid-air free surface. Such numerical scheme has been demonstrated to be able to capture the essential features of the free surface, even for the violent flow phenomenon as in sloshing [14]. The free surface of the liquid domain is first initialized using the level-set function. Based on the velocity field determined from the Navier-Stokes equations, the free surface (*i.e.* the level set function) is convected accordingly. As the free surface is displaced in the domain, it would not be possible to have the free surface always remained entirely aligned along the boundaries of the elements. In other words, there will be elements partially filled with liquid. This imposes a challenge in the treatment of the equilibrium between the hydrostatic forces and the representation of the pressure gradient, due to the discontinuity in the density across the liquid-gas interface. Such challenge is circumvented by using a pressure shape function enrichment scheme. The partially filled elements are locally refined so that the liquid-air interfaces can be represented exactly. Last but not least, a

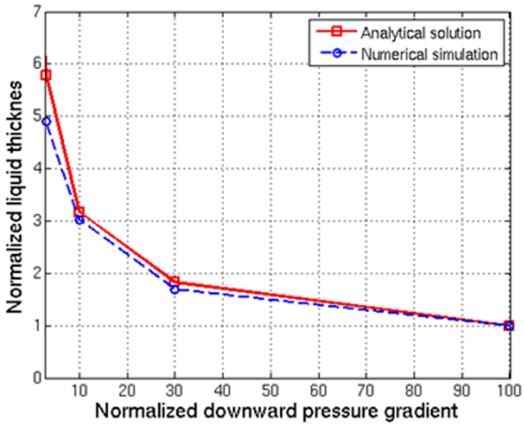

Figure 5: Comparison of analytical and simulated normalized liquid thickness as a function of the force adverse to the flow

matrix condensation procedure is employed to eliminate the new pressure variables prior to global matrix assembly. Such treatment preserves the structure of the global matrix, and greatly improves the efficiency of the solution process.

Adverse pressure gradient

The coupling of the gas jet wiping onto the liquid zinc film begins with the consideration of the effect of the adverse pressure gradient. As a start, a thin 3D domain, with only a few layers in Z, is employed. The line speed of 1 m/s is used. The effect of surface tension is not considered in the simulation. It is found that the adverse pressure gradient, which acts as an additional downward force in the liquid film, has a direct impact on the resulting thickness of the zinc coating. Figure 5 compares computed zinc film thickness for different values of the applied adverse force with those predicted by an analytical formula based on low speed continuous withdrawal theory, pioneered by Landau and Levich [15], [16]:

$$h = 0.944\left(\frac{\sigma}{\rho g}\right)^{1/2}\left(\frac{\mu U}{\sigma}\right)^{2/3}$$

where h is the final film thickness, σ the surface tension coefficient, ρ the density, g the gravitational acceleration, μ the dynamic viscosity, and U the strip moving velocity. The expression is valid for small $Ca = \mu U/\sigma < 0.03$ [16]. Because the analytical solution includes the surface tension and the numerical model does not, the values are normalized with respect to the thickness for the largest applied force. As can be seen, the computed thickness behaves in the same way as the analytical solution.

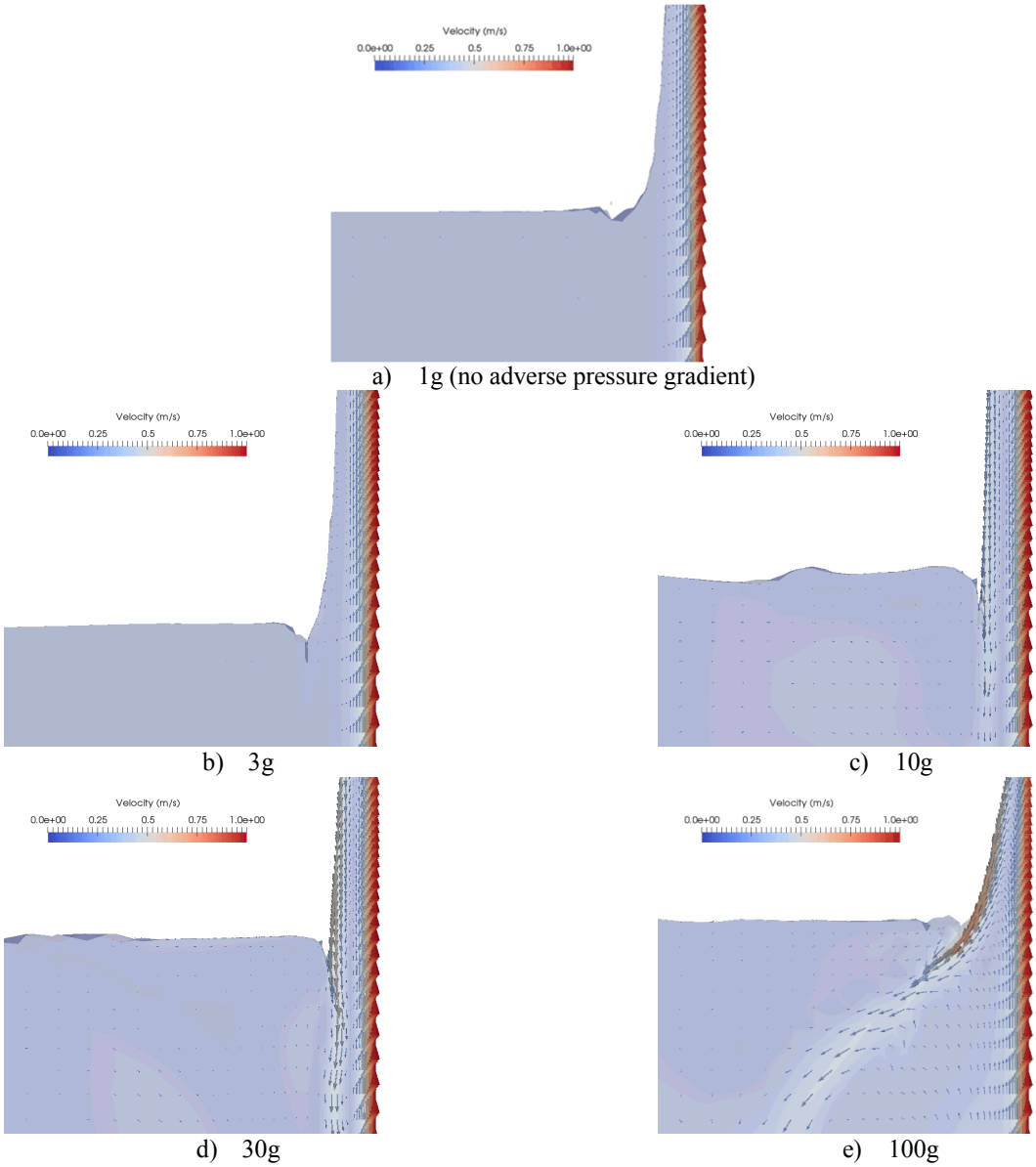

a) 1g (no adverse pressure gradient)

b) 3g

c) 10g

d) 30g

e) 100g

Figure 6: Liquid zinc entrainment along the steel strip

In Figure 6, the solutions for the cases where the force applied to the liquid is $1g$ (only gravity), $3g$, $10g$, $30g$, and $100g$ are shown. The effect of increased adverse force is shown to have a direct impact not only on the actual thickness of the liquid film on the strip, but also on the flow dynamics and the return of part of the liquid into the bath. This is illustrated by the velocity vectors in Figure 6. For the case without adverse forces, there is no return flow to the bath, whereas for larger adverse forces, a significant part of the entrained liquid is observed to returns to the bath. Moreover, simulations show that this return flow does not go along the bath surface, but instead penetrates through the free surface; thus bringing any oxides from the free surface into the interior of the zinc bath.

Liquid film model with shear stress from the gas jet

Next, the shear stress generated by the wiping gas jet onto the free surface of the adhered zinc film was applied as a boundary force on the liquid-air interface along the liquid zinc film. Figure 7 shows the applied shear rate distribution at the liquid-air interface in the numerical simulation obtained from the experimental work by Alibeigi [10] for $z/d = 6$. The fitting expression has good agreements.

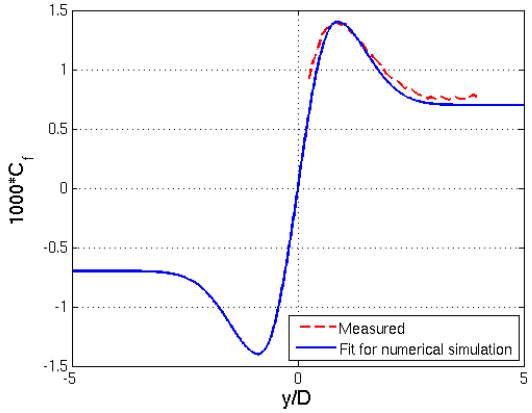

Figure 7: Shear stress: Measurement obtained from Alibeigi [10] for $z/d = 6$

The solution of the free surface problem coupling the liquid zinc entrainment along the steel strip and the effect of air-knife is illustrated in Figure 8. The steel strip surface is on the right hand side of each image and the interface with the flow from air-knife is on the left hand side. Note that the length scale in the Y direction (along the strip movement) was reduced by a factor of 10 in order to be able to visualize the coating thinning. This is equivalent to increasing the length scale in the thickness direction by a factor of 10. The solutions shown here clearly illustrate the effect of the shear stress in the thickness of the coating. The effect of the air knifes is quite rapid as it is visible even after 0.1 seconds. The coating thickness becomes stable with time after 0.4 seconds. Those solutions also indicate the dynamic of the flow when the coating thickness decreases as part of liquid returns toward the bath. The colors in each image are from the vertical velocity with upward velocities shown in red and downward velocities shown in blue. The flow direction is also indicated by the velocity vectors. At t=0s, there is not yet any effect from the shear stress and the liquid film only goes upward with the movement of the strip. Once the shear stress from the air-knife is imposed, a significant portion of the liquid is observed to flow downward toward the bath. In practice, this could have the implication of transferring of oxides formed at the air-zinc interface back into the galvanizing bath.

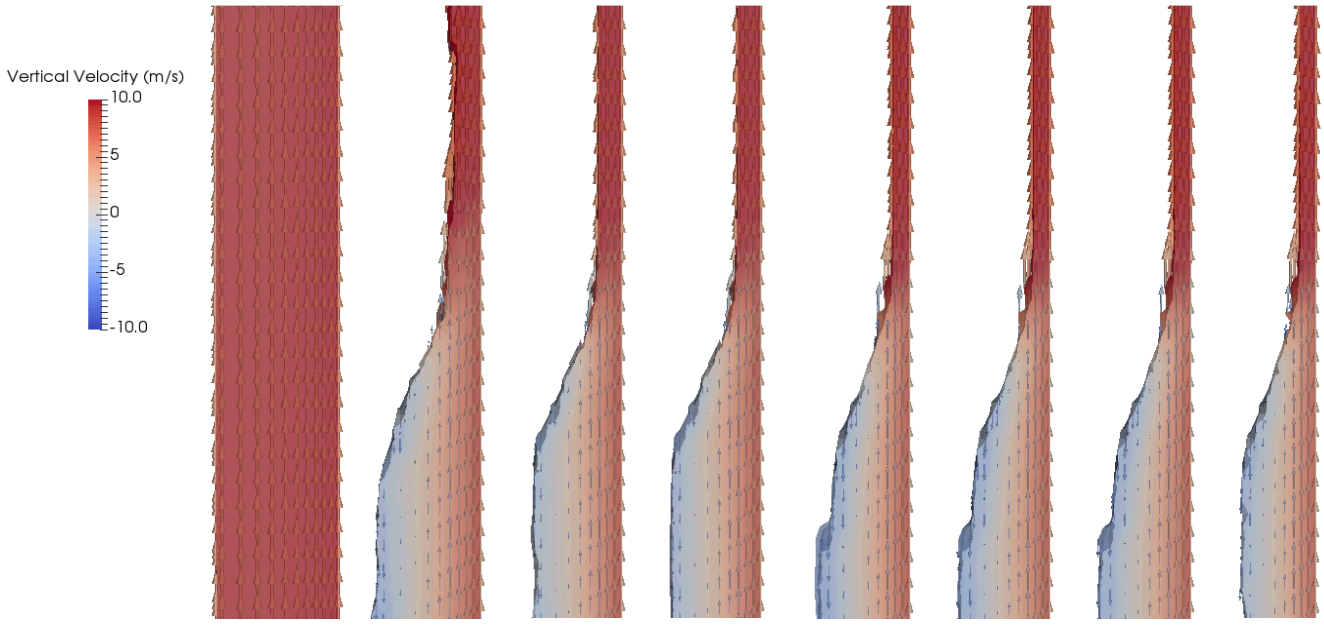

Figure 8: Transient solution of the coating thinning under the effect of the air-knife

SUMMARY AND FUTURE WORK

The present work reports the recent progress on the development of a three dimensional numerical model for the gas jet wiping process near the galvanizing bath surface for the investigation of top skimming formation. The model construction begins with the air-knife model, which determines the compressible turbulence flow field using SU2. The pressure profiles predicted from the simulation are in good agreement with measurements from an experimental work at two different stand-off distances. Then, the effects of the adverse pressure gradient and the shear stress from the turbulence jet onto the free surface of the liquid zinc film are modeled using an in-house finite element flow solver via a level-set approach. The effects of the coupling of the air-knife flow field onto the liquid zinc film are demonstrated.

Based on the preliminary simulation results, the present approach seems to be quite computational cost friendly. The development will continue to incorporate other key physical mechanisms of the gas jet wiping process and will extend fully to the three-dimensional case in the future.

ACKNOWLEGEMENT

The authors would also like to acknowledge the International Zinc Association, the sponsors of the Galvanized Autobody Partnership program ZCO-77 and the Advanced Manufacturing Program of NRC for making this work possible.

REFERENCES

[1] F. E. Goodwin and M. Dubois, “Review on wiping: A key process limiting CGL productivity,” presented at the AISTech - Iron and Steel Technology Conference Proceedings, 2012, pp. 1847–1859.
[2] M. Dubois, “Production of top skimmings in hot dip galvanizing,” *Rev. Métallurgie*, vol. 101, no. 7–8, pp. 569–575, Jul. 2004.
[3] J. Strutzenberger and R. Pree, *Generation of scum due to wiping in hot-dip galvanizing*. 2011.
[4] K. Myrillas, P. Rambaud, J.-M. Mataigne, P. Gardin, S. Vincent, and J.-M. Buchlin, “Numerical modeling of gas-jet wiping process,” *Chem. Eng. Process. Process Intensif.*, vol. 68, pp. 26–31, 2013.
[5] C. Pfeiler, W. Eßl, G. Reiss, C. K. Riener, G. Angeli, and A. Kharicha, “Investigation of the Gas-Jet Wiping Process − Two-Phase Large Eddy Simulations Elucidate Impingement Dynamics and Wave Formation on Zinc Coatings,” *Steel Res. Int.*, vol. 88, no. 9, 2017.
[6] J.-M. Buchlin, “Modelling of Gas-Jet Wiping,” in *Thin Liquid Films, and Coating Processes*, Belgium: von Karman Institute for Fluid Dynamics, 1997.
[7] F. Palacios *et al.*, “Stanford University Unstructured (SU2): An open-source integrated computational environment for multi-physics simulation and design,” in *51st AIAA Aerospace Sciences Meeting including the New Horizons Forum and Aerospace Exposition 2013*, 2013.
[8] T. D. Economon, F. Palacios, S. R. Copeland, T. W. Lukaczyk, and J. J. Alonso, “SU2: An open-source suite for multiphysics simulation and design,” *AIAA J.*, vol. 54, no. 3, pp. 828–846, 2016.
[9] T. D. Economon *et al.*, “Performance optimizations for scalable implicit RANS calculations with SU2,” *Comput. Fluids*, vol. 129, pp. 146–158, 2016.
[10] S. Alibeigi, “Experimental Investigation of Air-Knife Geometry in Continuous Hot-Dip Galvanizing,” McMaster University, Hamilton, Ontario, Canada, 2013.
[11] F. R. Menter, “Zonal two equation κ-ω turbulence models for aerodynamic flows,” in *AIAA 23rd Fluid Dynamics, Plasmadynamics, and Lasers Conference, 1993*, 1993.
[12] P. R. Spalart and S. R. Allmaras, “One-equation turbulence model for aerodynamic flows,” *Rech. Aerosp.*, no. 1, pp. 5–21, 1994.
[13] C. Geuzaine and J.-F. Remacle, “Gmsh: A 3-D finite element mesh generator with built-in pre- and post-processing facilities,” *Int. J. Numer. Methods Eng.*, vol. 79, no. 11, pp. 1309–1331, 2009.
[14] B. Blais, F. Ilinca, and K. R. Yu, “Solution of Complex Free Surface Flows using Enriched Pressure Shape Functions,” *Comput. Fluids*, Submitted for publication.
[15] L. Landau and B. Levich, “Dragging of a Liquid by a Moving Plate,” *Acta Physicochim. URSS*, vol. XVII, no. 1–2, 1942.
[16] J. A. Tallmadge and C. Gutfinger, “Entrainment of liquid films: Drainage, withdrawal, and removal,” *Ind. Eng. Chem.*, vol. 59, no. 11, pp. 18–34, 1967.